Available online at www.sciencedirect.com
SCIENCE DIRECT®

Journal of the European Ceramic Society 23 (2003) 1667–1674
www.elsevier.com/locate/jeurceramsoc

Diffusion induced grain-boundary migration and mechanical property improvement in Fe-doped alumina

Young-Woo Rhee[a], Ho Yong Lee[b], Suk-Joong L. Kang[a,*]

[a]*Materials Interface Laboratory, Department of Materials Science and Engineering, Korea Advanced Institute of Science and Technology, Taejon 305-701, South Korea*

[b]*Division of Metallurgy and Materials Engineering, Sunmoon University, Chungnam 336-840, South Korea*

Received 20 April 2002; received in revised form 23 October 2002; accepted 2 November 2002

Abstract

When 1 wt.%-Fe_2O_3-doped Al_2O_3 samples were sintered at 1600 °C in a reducing atmosphere, the additive remained as Fe precipitates at the triple grain-junctions. On annealing the sintered samples in an oxidizing atmosphere, however, the Fe precipitates dissolved into the Al_2O_3 grains at the surface region and induced grain-boundary migration. This diffusion induced grain-boundary migration (DIGM) resulted in the corrugation of grain boundaries and the formation of misfit dislocations in the migration region. The mechanical properties of the samples were evaluated by the Hertizian indentation technique under static and cyclic loading. The sample with DIGM showed better mechanical properties than that without DIGM: improvement in the critical load for cone crack initiation under static loading and in the number of cycles for crack initiation under cyclic loading. In terms of microstructure, the cone crack propagation was suppressed and a quasi-plastically deformed region appeared under static loading, and the surface chipping at the contact area was much reduced under cyclic loading. An insignificantly low value of residual stresses at the surface of the sample with DIGM suggested that the mechanical property improvement was due to the microstructural changes, the grain boundary corrugation and the misfit dislocations, rather than to any compressive stresses introduced in the migration layer. DIGM appears to be a possible means of improving the mechanical properties of Al_2O_3.

Keywords: Al_2O_3; DIGM; Grain boundaries; Mechanical properties; Sintering

1. Introduction

When a polycrystalline solid becomes chemically unstable at high temperatures, equilibration reactions forming a new solid solution in chemical equilibrium occur. Sometimes the equilibrating reactions do not occur by conventional lattice diffusion but rather by boundary migration accompanied by boundary diffusion, forming a new solid solution behind the migrating boundaries. This phenomenon is referred to as *diffusion induced grain-boundary migration* (DIGM) or *chemically induced grain-boundary migration* (CIGM).[1–5] DIGM has been found in a number of systems,[1–5] including alumina with the solute elements Cr_2O_3 and Fe_2O_3.[6–12] For the Al_2O_3–Fe_2O_3 system, the increase in Fe_2O_3 solubility caused by temperature change or atmosphere change from reducing to oxidizing induced a grain boundary migration as a result of a discontinuous dissolution of iron aluminate spinel precipitates.[9,12]

In terms of microstructure, DIGM often results in the undulation of the grain boundaries[1–5] and the formation of misfit dislocations.[1] These microstructural changes of grain boundary undulation and misfit dislocation formation are expected to alter the fracture behavior of the material, such as fracture mode and toughness. In fact, Harmer et al.[13] reported that grain boundary undulation caused a change in the fracture mode from intergranular to transgranular in strontium calcium ferrite. A similar change in fracture mode and an increase in fracture toughness were also observed in lanthanum-modified lead zirconium titanate (PLZT) after DIGM.[14]

The purpose of the present investigation was to study diffusion induced grain-boundary migration and its effect on the mechanical properties of alumina, a material of

* Corresponding author. Tel.: +82-42-869-4113; fax: +82-42-869-8920.
E-mail address: sjkang@mail.kaist.ac.kr (S.-Joong L. Kang).

0955-2219/02/$ - see front matter © 2003 Elsevier Science Ltd. All rights reserved.
PII: S0955-2219(02)00400-4

practical importance. The grain-boundary migration was induced in Fe_2O_3-containing Al_2O_3 samples by controlling the sintering and annealing atmospheres. The effect of DIGM on the mechanical properties was compared and analyzed using the Hertzian indentation technique in samples with and without grain-boundary migration layers.

2. Experimental procedure

Samples of $99Al_2O_3$–$1Fe_2O_3$ (wt.%) were prepared from Al_2O_3 (AKP-50 Sumitomo Chemicals, Osaka, Japan; 99.99 wt.% in purity) and $Fe(NO_3)_2{\cdot}9H_2O$ (Shinyo Pure Chemicals, Osaka, Japan; 99.9 wt.% in purity) powders. The proportioned powder mixture was wet-milled for 12 h in ethyl alcohol using a polyethylene bottle and high purity alumina balls. The dried slurry was isostatically pressed under 200 MPa into bars of $\sim 5\times5\times21$ mm in size. The compacts were calcined at 800 °C for 2 h to decompose the nitrate and then sintered at 1600 °C for 2 h in $95N_2$–$5H_2$. The sintered samples were ground and polished to a 3-μm finish. Some of the polished samples were annealed at 1500 °C for 2 h in air and others at 1500 °C for 2 h in the same atmosphere as the sintering atmosphere of $95N_2$–$5H_2$. For the annealing, all of the samples were rapidly heated to the annealing temperature and cooled to room temperature at about 200 K/min by using a sample pusher in order to minimize possible microstructural change during the heating and cooling.

Microstructures of the sintered and annealed samples were observed on their polished sections without further treatment using a scanning electron microscope (SEM) and a transmission electron microscope (TEM). The cation concentrations in the grains were measured with an energy dispersive spectroscopy (EDS) attached to the TEM. The residual stresses remaining at the surface of the annealed samples were measured by X-ray diffraction ($\sin^2\psi$ method) after polishing the surface with 1 μm diamond paste. To obtain the lattice strains, the (416) plane of alumina was chosen. In our case the effective depth of penetration (95%) was estimated to be $\sim$110 μm. The residual surface stress was calculated by using the measured lattice strain and the X-ray elastic constants of alumina (416) planes: $E_{416} = 304$ GPa, and $\nu_{416} = 0.2$.[15]

The mechanical properties of the annealed samples were evaluated using the Hertzian indentation technique after polishing them to a 1-μm finish to remove thermal grooves. Single-cycle indentations with a peak load up to $P = 2500$ N and at a fixed cross-head speed of 0.2 mm/min were made on the polished surfaces using a tungsten carbide (WC) sphere of radius $r = 3.18$ mm. Critical loads for cone crack initiation were measured by making sequential indentations at incrementally increasing loads in the vicinity of the threshold along rows in the sample surface, with a minimum five indentations at each prescribed load. Multi-cyclic indentations were also made in air with a relative humidity of ≈50% using a servo-hydraulic universal testing machine. The cyclic tests were run in repeat loading in haversinusoidal waveform up to 10^5 cycles at frequency $f = 10$ Hz, between the specified maximum and minimum loads (the latter typically 20 N, primarily to prevent the contact from wandering). The indented surfaces were examined by optical microscopy (Nomarski interference).

In addition to the Hertzian indentation tests, four-point flexural strengths were also measured using bar samples of $\sim 3\times4\times16$ mm with an inner span of 6.35 mm (1/4 inch) and an outer span of 12.7 mm (1/2 inch) at a constant crosshead speed of 20 mm/min. Before the test, the edges of the samples were prechamfered to minimize edge failures. At least five samples were tested for each experimental condition.

3. Results and discussion

All of the $99Al_2O_3$–$1Fe_2O_3$ samples were densified to more than 98% relative density after sintering and annealing. Fig. 1(a) shows the typical microstructure of a polished section of the sample annealed at 1500 °C for 2 h in $95N_2$–$5H_2$ after sintering at 1600 °C for 2 h in $95N_2$–$5H_2$. The sample consists of equiaxed corundum grains with an average size of $\sim$15 μm. Fig. 1(b) shows the surface microstructure of the sample annealed at 1500 °C for 2 h in air after sintering in $95N_2$–$5H_2$. Grain boundary migration occurred at the sample surface during the annealing in air and most of the grain-boundaries became wavy and curved, as in previous investigations.[9,12] The average grain size of this sample, however, was similar to that of the sample annealed in $95N_2$–$5H_2$ [Fig. 1(a)]. It appears that the grain size does not vary with different annealing atmospheres, $95N_2$–$5H_2$ or air, in the studied experimental condition.

According to the Al_2O_3–Fe_2O_3 system,[16–19] the solubility of Fe_2O_3 in Al_2O_3 decreases with a decreasing oxygen partial pressure. The solubility is $\sim$15 wt.% at 1500 °C in air (0.2 atm O_2); however, it is $\sim$3 wt.% at the oxygen partial pressure P_{O_2} of $\sim$0.03 atm. In the $95N_2$–$5H_2$ atmosphere with a P_{O_2} of less than 10^{-14} atm at 1500 °C, the solubility of Fe_2O_3 must be much lower than 3 wt.%. In the $95N_2-5H_2$-sintered samples, many second phase particles of 0.2–1 μm in size were, indeed, observed at the grain boundaries and triple junctions, as shown in Fig. 2 of the bright field TEM micrograph. The electron diffraction pattern (insert) of the second phase particle in this figure coincides with that of α-Fe from the [001] zone, showing that the second phase particle is α-Fe. This result is in good agreement with a

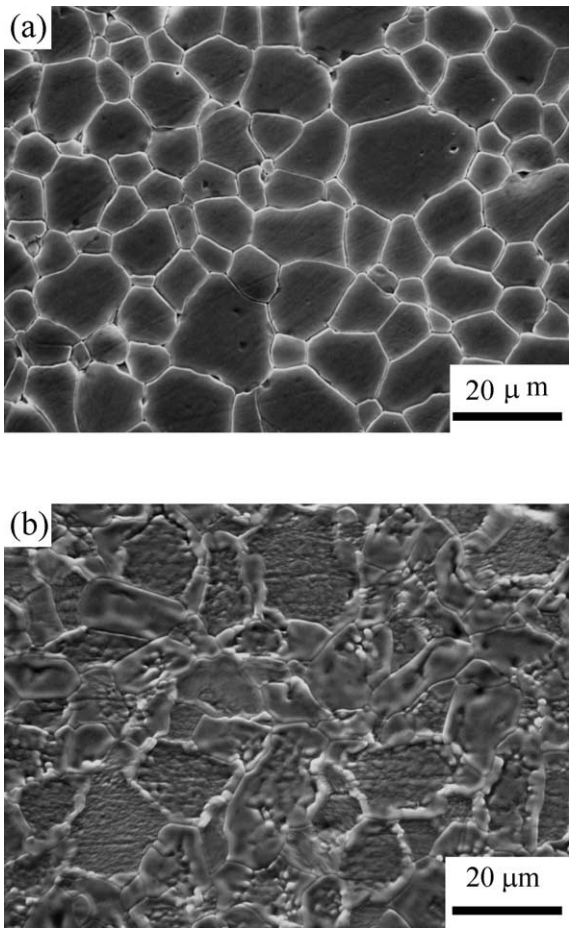

Fig. 1. SEM micrographs of the $99Al_2O_3$–$1Fe_2O_3$ (wt.%) sample sintered at 1600 °C for 2 h in $95N_2$–$5H_2$ and then annealed at 1500 °C for 2 h (a) in $95N_2$–$5H_2$ and (b) in air.

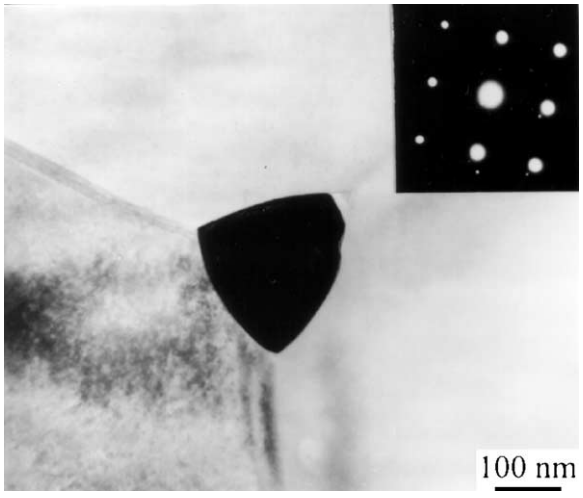

Fig. 2. TEM micrograph of an α-Fe precipitate in the $99Al_2O_3$–$1Fe_2O_3$ sample sintered at 1600 °C for 2 h in $95N_2$–$5H_2$ and then annealed at 1500 °C for 2 h in $95N_2$–$5H_2$. The insert is a diffraction pattern of the α-Fe precipitate with a [001] zone axis.

previous investigation[19] which showed that the corundum phase with less than 1 mol.% Fe_2O_3 and metallic Fe are stable phases at 1500 °C under $P_{O_2} = 5\times10^{-11}$ atm.

In the sample annealed in air, no more α-Fe precipitates were present at the grain boundaries and triple junctions of the surface region. Instead, a number of dislocations were formed in the migrated region, as shown in Fig. 3. The dotted line "O" in Fig. 3 delineates the original position of the grain boundary. A distinct line denoted by "M" is the final position of the grain boundary after the migration. The two electron diffraction patterns (inserts) of the original grain and the migration region coincide with those of α-Al_2O_3 from the [0001] zone, showing that the two regions have the same crystallographic orientation.

Fig. 4 plots the measured Fe ion concentration among the total cations (Al and Fe ion) in the migrated region and the two original corundum grains in Fig. 3. A concentration discontinuity is observed between the migrated region and the original grains: ~3.3 at% of Fe in the migrated region and ~0.2 at% in the original grains. The abrupt increase in Fe concentration [Fe/(Fe + Al)] in the migrated region in Fig. 4 and the dislocations observed in the migrated region in Fig. 3 show that the grain boundary migration was accompanied by the dissolution of Fe ions into the corundum grains and resulted in the formation of misfit dislocations. Therefore, when the sample sintered in $95N_2$–$5H_2$ is annealed in air where Fe solubility in Al_2O_3 is higher than in the sintering atmosphere, a diffusion induced grain-boundary migration (DIGM) occurs with the dissolution of Fe precipitates; this is similar to the previously observed DIGM in Al_2O_3 as a result of the discontinuous dissolution of iron aluminate spinel.[12]

However, the DIGM occurred only in the surface region with a layer thickness of ~200 μm, as shown in Fig. 5. This DIGM layer thickness was nearly unchanged with increased annealing time up to 8 h. (The thickness after 8 h annealing was ~210 μm.) Considering the relatively high grain-boundary diffusivity of oxygen in alumina, $\sim10^{-5}$ cm^2/s at 1500 °C, with a diffusion thickness of 10^{-7} cm,[20,21] the oxygen diffusion during the air-annealing is unlikely to be responsible for this thickness limitation of the DIGM layer. When the iron precipitates with a molar volume of 7.09 cm^3 oxidize to Fe_2O_3 (30.4 cm^3/mol) and then dissolve into the corundum grains (25.6 cm^3/mol), the net volume change by the dissolution and alloying of Fe is an increase of ~0.35 vol%. The elastic strain energy due to the volume increase appears to be high enough to suppress the oxidation and the alloying of Fe inside the samples as in the case of the suppression of $FeAl_2O_4$ dissolution in Al_2O_3.[9] In fact, any transformation which causes a volume increase may be suppressed inside a rigid solid matrix by the introduction of strain energy.[22] As the

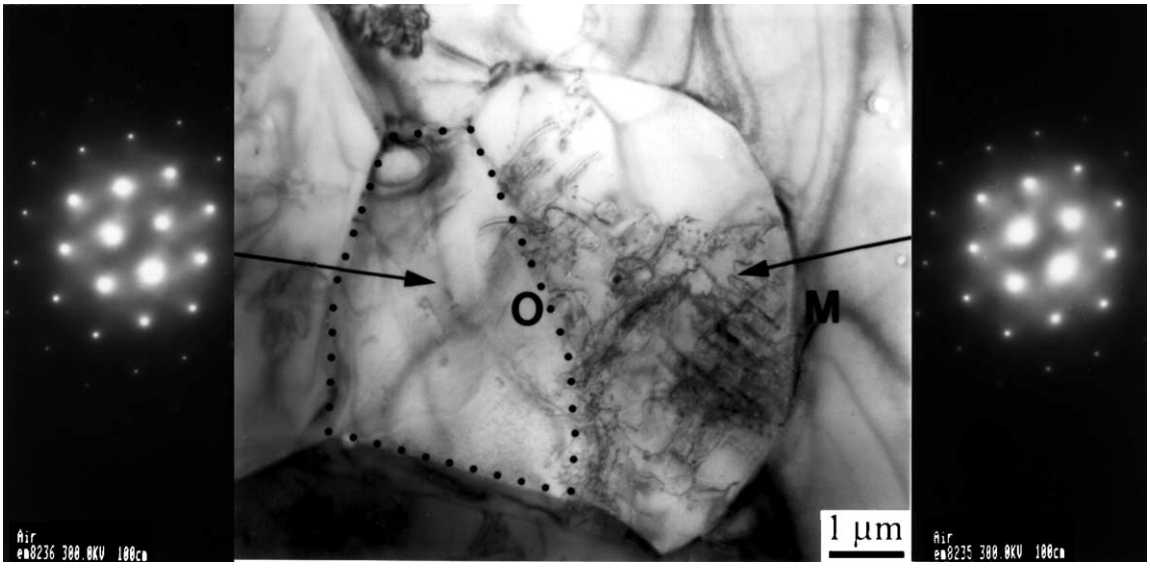

Fig. 3. TEM micrograph of the $99Al_2O_3$–$1Fe_2O_3$ sample sintered at 1600 °C for 2 h in $95N_2$–$5H_2$ and then annealed at 1500 °C for 2 h in air. The inserts are the diffraction patterns of the original grain and the migrated region with a [0001] zone axis.

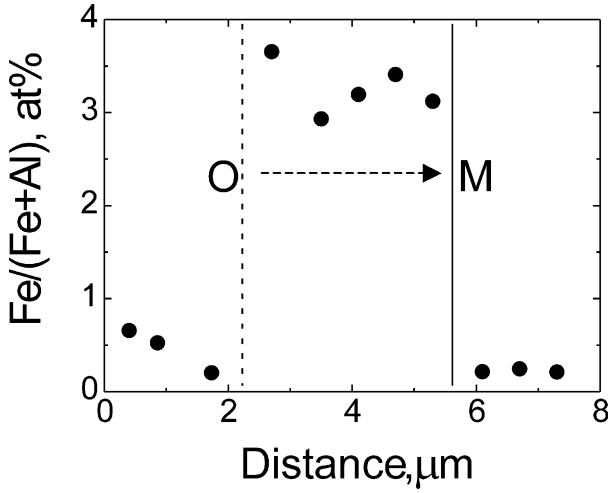

Fig. 4. Measured Fe ion concentrations in the migrated region and original corundum grains in Fig. 3. The dotted and solid lines show the initial and final positions of the grain boundary.

formation and dissolution of Fe_2O_3 are suppressed, the grain boundaries do not migrate. On the contrary, at the surface where the volume increase may be accommodated at a high temperature, the oxidation of Fe at the grain boundary appears to be possible and results in the migration of the grain boundary by the supply of Fe_2O_3, as shown in Fig. 1(b). Therefore, we attribute the thickness limitation of the DIGM layer to the suppression of the oxidation and alloying of Fe because of the volume expansion.

The effect of the surface modification on mechanical properties was examined using the Hertzian indentation tests of the annealed samples in either $95N_2$–$5H_2$ or air. The Hertzian indentation technique uses flaws with a depth of a few microns and gives results relevant to the properties in the short crack regions.[23] Thus, this technique is very useful for evaluating the surface layer properties of materials. In addition, Hertzian contact stress fields are theoretically very well defined and stress fields are concentrated in the near contact area.[24–27] For the $95N_2$–$5H_2$-annealed sample with a typically polycrystalline microstructure, a Hertzian cone crack initiated at 1000 N. On the other hand, cracks were found above 1200 N in the air-annealed sample with a DIGM layer. The critical load for cone crack initiation increased by approximately 200 N via the surface modification with DIGM.

Fig. 6 shows the vertical sections of the two kinds of samples after indentation with a 2000 N load. The samples were prepared by the bonded interface technique.[27,28] Without the DIGM layer [Fig. 6(a)], the cone crack was well developed and a few microcracks were shown in the sub-surface region. However, in the sample with a DIGM layer [Fig. 6(b)], the cone crack propagation was strongly suppressed and a quasi-plastic deformation occurred in the sub-surface region, mostly below the DIGM layer, indicating that the DIGM layer changed the fracture behavior of the sample. It appears that the suppression of the cone crack propagation resulted in the formation of a quasi-plastically deformed region below the DIGM-strengthened layer.

Not only the static property but also the cyclic property was improved by introducing a surface DIGM layer. Fig. 7 shows the surface damage evolution during the cyclic indentation tests under a $P = 1000$ N load of the two different samples with and without a DIGM layer. A surface ring crack forms at the first cyclic loading and the damage becomes more severe with increasing contact cycles in the $95N_2$–$5H_2$-annealed sample without DIGM. On the other hand, for the air-

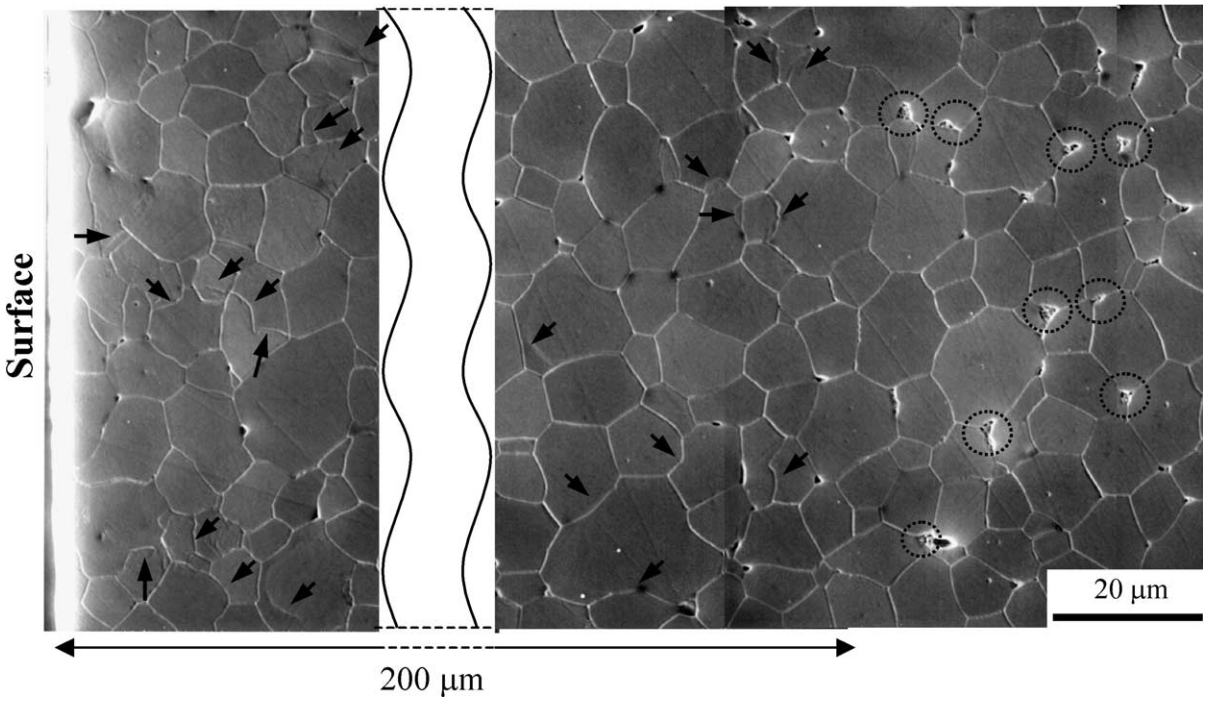

Fig. 5. Vertical section showing a DIGM layer formed in the $99Al_2O_3-1Fe_2O_3$ sample during annealing at 1500 °C for 2 h in air. The section was thermally etched at 1500 °C for 10 min in H_2. Arrows indicate migration boundaries and circles show undissolved Fe precipitates in the interior of the sample.

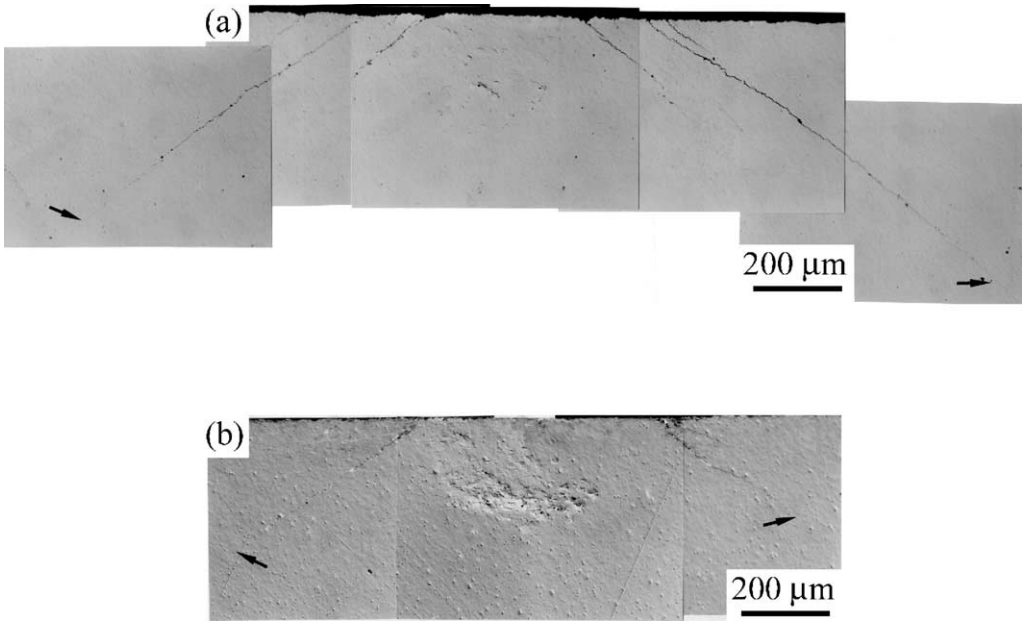

Fig. 6. Section views of the surface damages formed with $P = 2000$ N in the samples sintered and annealed at 1500 °C for 2 h (a) in $95N_2$–$5H_2$ and (b) in air. Arrows indicate the cone crack tips.

annealed sample with a DIGM layer, a surface ring crack does not develop until 10^2 cycles but is observed after 10^3 cycles.

Fig. 8 shows the surface damage micrographs and the 4-point flexural strengths of the two kinds of samples after indentation of 10^4 cycles at $P = 1000$ N. For comparison, the flexural strengths of unindented samples are also presented. For the $95N_2$–$5H_2$-annealed samples without DIGM layers, the mean strength drops from 297 MPa to 254 MPa after 10^4-cycle-indentation. By contrast, the average strength of the air-annealed samples with DIGM does not essentially degrade at all: 345 MPa for unindented samples and 342 MPa for 10^4-cycle-indented samples. The difference in the flexural

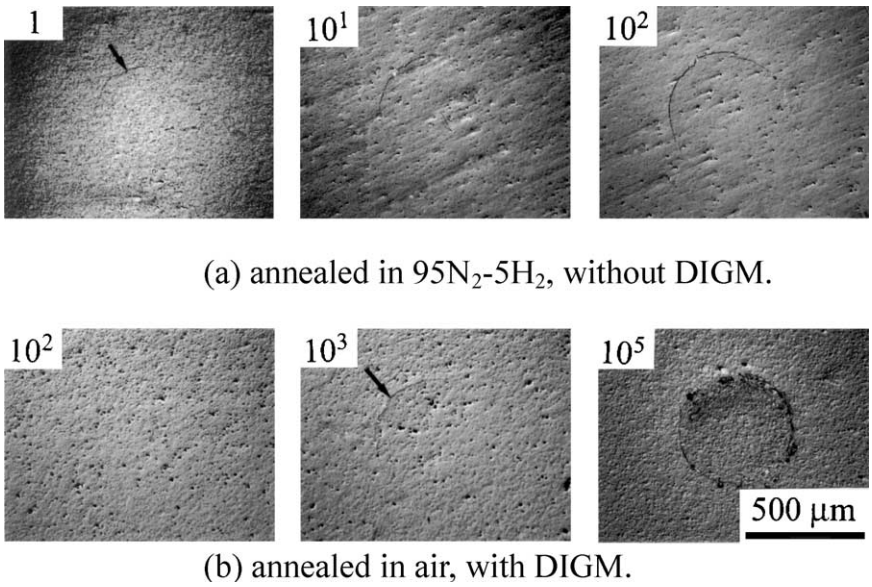

Fig. 7. Surface damages formed during an increase in contact cycles with $P = 1000$ N in the samples sintered at 1600 °C for 2 h in $95N_2$–$5H_2$ and then annealed at 1500 °C for 2 h (a) in $95N_2$–$5H_2$ and (b) in air. The figures on the micrographs denote the number of contact cycles.

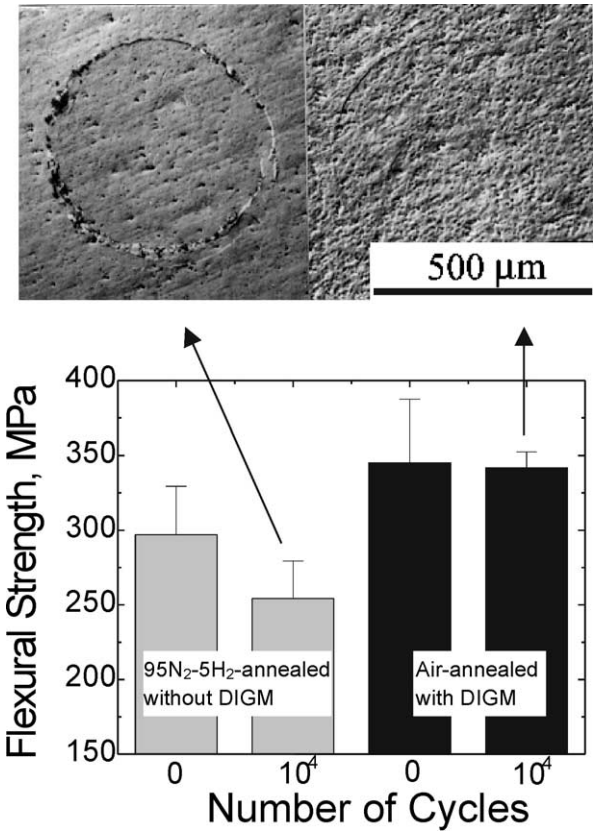

Fig. 8. Flexural strengths before and after an indentation test of 10^4 cycles with $P = 1000$ N for the samples sintered at 1600 °C for 2 h in $95N_2$–$5H_2$ and then annealed at 1500 °C for 2 h in $95N_2$–$5H_2$ or in air. The micrographs show the surface damages after the indentation test.

strength after 10^4 cycles must be related to the difference in surface damage. Compared to the sample without DIGM, much smaller cracks and much less chipping near the contact area are observed in the sample with a DIGM layer. The results shown in Figs. 7 and 8 thus demonstrate that the sample with a DIGM layer is much more damage-tolerant at cyclic loading.

The observed improvement in the cyclic property by DIGM must be related to the increase in the critical load for cone crack initiation. The increase in the critical load may result from the residual stresses stored in the DIGM layer because of the dissolution of Fe and also the difference in the thermal expansion coefficient between the surface layer and the sintered body. A previous investigation,[29] however, suggested that the thermal expansion mismatch does not result in compressive stresses in an Al_2O_3–Fe_2O_3 system. On the other hand, the Fe dissolution results in a volume expansion and compressive stresses in the DIGM layer. The compressive stresses remaining at the surface were measured to be ~14 MPa by XRD ($\sin^2\psi$ method[15]).

The measured compressive stress, however, does not account for the increase in the critical load for cone crack initiation by 200 N. As a rough calculation,[25] this critical load increase corresponds to a ~265 MPa increase in compressive stress. This value is obviously much larger than the measured compressive stress of ~14 MPa. It appears, therefore, that the surface DIGM layer with corrugated grain boundaries and misfit dislocations suppresses the flaw from propagating in the initial propagation stage, as shown in Fig. 6(b), and that the strength of the layer is stronger than that without DIGM. Fig. 9 shows the fracture surfaces of the two kinds of samples after the bending test. Without the DIGM layer [Fig. 9(a)], the fracture mode is intergranular, as observed in conventional alumina ceramics.[30] However, a transgranular fracture mode is introduced in the DIGM layer [Fig. 9(b)]; this suggests

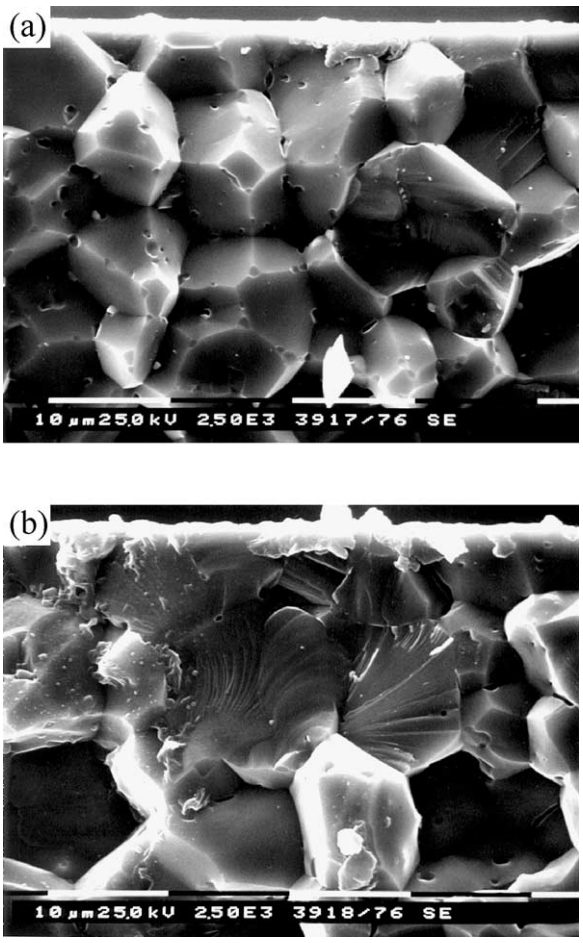

Fig. 9. Fractographs of the surface region in the samples sintered at 1600 °C for 2 h in $95N_2$–$5H_2$ and then annealed at 1500 °C for 2 h (a) in $95N_2$–$5H_2$ or (b) in air.

that the DIGM layer improved the grain-boundary strength. The increase in the critical load for cone crack initiation can, therefore, be attributed to the improvement of the grain-boundary strength, which would be related to the presence of misfit dislocations and the corrugated shape of the grain boundaries in the DIGM layer.

4. Conclusions

In the present investigation, we studied the diffusion induced grain boundary migration (DIGM) of alumina and its effect on mechanical properties. By controlling the sintering and annealing atmospheres, it was possible to prepare two types of Fe-containing alumina samples with distinctly different surface microstructures, one with a typically polycrystalline microstructure and the other with a DIGM layer of ~200 μm. A number of misfit dislocations formed in the migrated regions of the DIGM layer. The surface modification by DIGM suppressed the cone crack propagation and improved the critical load for cone crack initiation by 200 N in single-cycle Hertzian indentation tests and increased greatly the number of cycles for cone crack formation in multi-cycle Hertzian indentation tests.

The measured flexural strength of the two types of samples and the measured compressive stresses in the surface layer showed that the compressive stresses did not account for the observed improvement in mechanical properties. It appears, therefore, that the initial propagation of surface flaws is suppressed by a surface DIGM-modified layer and that the DIGM layer improved the strength of the material. These results can be attributed to the undulated shape of the grain boundaries and the presence of the misfit dislocations in the migration layer. The present alumina example may suggest general applicability of a DIGM technique for improving mechanical properties of other structural ceramics.

Acknowledgements

Helpful comments of Dr. Brian Lawn at NIST and Professor Do Kyung Kim at KAIST are acknowledged. The cyclic Hertzian indentation tests were performed at the National Institute of Standards and Technology, Gaithersburg, USA. Supported by the National Research Laboratory (NRL) Program of the Ministry of Science and Technology in Korea.

References

1. Hillert, M. and Purdy, G. R., Chemically induced grain boundary migration. *Acta Metall.*, 1978, **26**, 333–340.
2. King, A. H., Diffusion induced grain boundary migration. *Inter. Mater. Rev.*, 1987, **32**, 173–189.
3. Handwerker, C. A., Diffusion-induced grain boundary migration in thin films. In *Diffusion Phenomena in Thin Films and Microelectronic Materials*, ed. D. Gupta and P. S. Ho. Noyes Publications, Park Ridge, NJ, 1988, pp. 245–322.
4. Yoon, D. Y., Chemically induced interface migration in solids. *Annu. Rev. Mater. Sci.*, 1989, **19**, 43–58.
5. Yoon, D. Y., Theories and observations of chemically induced migration. *Int. Mater. Rev.*, 1995, **40**(4), 149–179.
6. Lee, H.-Y. and Kang, S.-J. L., Chemically induced grain boundary migration and recrystallization in Al_2O_3. *Acta Mater.*, 1990, **38**, 1307–1312.
7. Lee, H.-Y., Kang, S.-J. L. and Yoon, D. Y., The effect of elastic anisotropy on the direction and faceting of chemically induced grain boundary migration in Al_2O_3. *Acta Mater.*, 1993, **41**, 2497–2502.
8. Lee, H.-Y., Kang, S.-J. L. and Yoon, D. Y., Coherency strain energy and the direction of chemically induced grain boundary migration in Al_2O_3–Cr_2O_3 and Al_2O_3–Fe_2O_3. *J. Am. Ceram. Soc.*, 1994, **77**, 1301–1306.
9. Lee, H. Y., Paek, Y. K., Lee, B. K. and Kang, S.-J. L., Discontinuous dissolution of iron aluminate spinel in the Al_2O_3–Fe_2O_3 system. *J. Am. Ceram. Soc.*, 1995, **78**(8), 2149–2152.
10. Han, S. C., Yoon, D. Y. and Brun, M. K., Migration of grain

boundaries in alumina induced by chromia addition. *Acta Mater*., 1995, **43**, 977–984.
11. Paek, Y. K., Lee, H.-Y. and Kang, S.-J. L., Direction of chemically induced interface migration in Al_2O_3-anorthite system. *J. Am. Ceram. Soc*., 1996, **79**, 3029–3032.
12. Lee, H. Y., Rhee, Y.-W. and Kang, S.-J. L., Discontinuous dissolution and grain-boundary migration in Al_2O_3–Fe_2O_3 by oxygen partial pressure change. *J. Am. Ceram. Soc*., 1996, **79**(6), 1659–1663.
13. Chang, E. K., Wang, Z. Y., Smyth, D. M. and Harmer, M. P., The 88th American Ceramic Society Annual Meeting Ceramographic Exhibit; cf. the back cover of the *J. Am. Ceram. Soc*., 1986, **69**[10].
14. Kim, J. J. and Kim, D. Y., Change in the fracture mode of PLZT ceramics by chemically induced grain-boundary migration. *J. Am. Ceram. Soc*., 1988, **71**(5), C228–C229.
15. Eigenmann, B., Scholtes, B. and Macherauch, E., Determination of residual stresses in ceramics and ceramic-metal composites by X-ray diffraction methods. *Mater. Sci. Eng*., 1989, **A118**, 1–17.
16. Levin, E. M., Robbins, C. R. and McMurdie, H. F., Figs. 27–35. In *Phase Diagrams for Ceramists*, ed. M. K. Reser. American Ceramic Society, Columbus, OH, 1964.
17. White, J., The relationship of phase diagrams to constitution and microstructure in ceramic and ceramic-metal systems. In *Phase Diagrams: Materials Science And Technology, Vol. 2*, ed. A. M. Alper. Academic Press, New York, 1970, pp. 21–66.
18. Muan, A. and Osborn, E. F., *Phase Equilibria among Oxides in Steelmaking*. Addison-Wesley, Reading, MA, 1965.
19. Meyers, C. E., Mason, T. O., Petuskey, W. T., Halloran, J. W. and Bowen, H. K., Phase equilibria in the system Fe–Al–O. *J. Am. Ceram. Soc*., 1980, **63**(11-12), 659–663.
20. Wang, H. A. and Kröger, F. A., Chemical diffusion in polycrystalline Al_2O_3. *J. Am. Ceram. Soc*., 1980, **63**(11-12), 613–619.
21. Dörre, E. and Hübner, H., *Alumina: Processing, Properties and Applications*. Springer-Verlag Berlin, Heidelberg, 1984.
22. Raj, R. and Lange, F. F., Crystallization of small quantities of glass (or a liquid) segregated in grain boundaries. *Acta Metall*, 1981, **29**, 1993–2000.
23. Franco, A., Roberts, S. G. and Warren, P. D., Fracture toughness, surface flaw sizes and flaw densities in Al_2O_3. *Acta Mater*., 1997, **45**(3), 1009–1015.
24. Frank, F. C. and Lawn, B. R., On the theory of Hertzian fracture. *Proc. Roy. Soc. Lond*., 1967, **A299**, 291–306.
25. Lawn, B. R. and Wilshaw, T. R., Indentation fracture: principles and applications. *J. Mater. Sci*., 1975, **10**, 1049–1081.
26. Lawn, B. R., *Fracture of Brittle Solids*. Cambridge University Press,, Cambridge, UK, 1993.
27. Lawn, B. R., Indentation of ceramics with spheres: a century after Hertz. *J. Am. Ceram. Soc*., 1998, **81**(8), 1977–1994.
28. Guiberteau, F., Padture, N. P. and Lawn, B. R., Effect of grain size on Hertzian contact in alumina. *J. Am. Ceram. Soc*., 1994, **77**(7), 1825–1831.
29. Frasier, J. T., Jones, J. T., Raghavan, K. S., McGee, T. D. and Bell, H., Chemical strengthening of Al_2O_3. *Am. Ceram. Soc. Bull*., 1971, **50**, 541–544.
30. Swanson, P. L., Fairbanks, C. J., Lawn, B. R., Mai, Y.-W. and Hockey, B. J., Crack-interface grain bridging as a fracture resistance mechanism in ceramics: I, experimental study on alumina. *J. Am. Ceram. Soc*., 1987, **70**(4), 279–289.